PNAS

Supporting Information for

Exploring the Activation Mechanism of Metabotropic Glutamate Receptor 2

Xiaohong Zhu, Mengqi Luo, Ke AN, Danfeng Shi, Tingjun Hou , Arieh Warshel, Chen Bai

Arieh Warshel, Tingjun Hou, Chen Bai
Email: warshel@usc.edu, baichen@cuhk.edu.cn, tingjunhou@zju.edu.cn

This PDF file includes:

S1. Simulation Methods

S1.1 Modeling the complexes

In this work, we used experimental crystal structures together with homology modeling technique to model the inactive (PDB ID:7EPA) state, the agonist-bound (PDB ID:7EPB) state, and the active state (PDB ID:7E9G) for calculations.

The VFT domains undergo a sequential conformational change, while the 7TM domains exhibit a substantial rearrangement from an inactive (S1) to an agonist-bound (S2) state with diverse dimerization patterns. Firstly, we directly used the targeted molecular dynamic (TMD) method to connect these two states, which leads to collisions between 7TM domains. This phenomenon indicates that the rotation of 7TMs forms a coupled relationship instead of occurring synchronously.

In order to avoid collisions, we disassembled the mGlu2 dimer, and used the TMD method to obtain the intermediate structures of these two subunits from S1 to S2. Then, USCF Chimera(1) was employed to assemble the two subunit intermediates. After obtaining these intermediate structures between S1 and S2, we added membrane particles and performed relaxation runs on each structure until the energy is converged. Then we trimmed the all-atom structures into coarse grained (CG) representations and evaluated their CG free energy to obtain the conformational free energy change profile (Figure 2a in the main text). Each point in Figure 2a represents a possible conformational state and its corresponding folding free energy.

Furthermore, to study how agonists bind to mGlu2, we take four parameters into account: the conformations of L subunit and R subunit in mGlu2 homodimer, and the agonist position for L and R subunit. In order to differentiate the conformational state of single subunit, the start-point and the end-point subunit states were numbered as subunit 0 and subunit 16, and the generated 15 intermediate conformations were numbered as subunit 1-15. Therefore, a total of 17 subunit states were applied to construct the conformations of mGlu2. For the agonist position, we generated the agonist binding free energy profile by docking an agonist at different distance away from the binding pocket in the VFT domain to the bulk solvent in one subunit of the mGlu2 dimer. Totally 25 structures were generated for each subunit state and we numbered each intermediate structure from 25 (agonists in the binding pocket) to 0 (agonists in the bulk solvent). Based on these, another agonist was also docked at different distance away from the binding pocket to the bulk solvent on the other subunit of the mGlu2 dimer. Then the subunit states of the conformations of mGlu2 and the agonist positions were combined to represent the process of the agonist binding to mGlu2 by four numbers. For example, the start-point was named as S (0, 0, 0, 0). Thus, a total of 195,364 (17*17*26*26) mGlu2 conformations were constructed. In this work, each state can be depicted as S (x, y, z, i) with x, y, ranging from 0 to 16, while z and i ranging from 0 to 25. Here x, y represent the conformational change of the L and R subunit of mGlu2 dimer, z, i indicate the agonist position for the R and L subunit.

The free energy landscape we obtained is shown in the main text Figure 4. The free energy corresponding to each point in Figure 4 is the sum of the conformational free energy and the agonist binding free energy. In addition, we also considered the situation when only one agonist binds to mGlu2, and the corresponding figures are shown in Figure S4 and S5.

In order to learn how the G_i protein induces the conformational changes of mGlu2, the structure of G_i protein in the G_i^{GDP} state (PDB ID: 6CRK) was "repaired" by using Modeller(2, 3). Then, HDOCK protein-protein docking (4) was performed to obtain the optimal binding pose of G_i protein to mGlu2 in the S2 state. For the structure of the G_i protein in the S3 state, we employed the active state of mGlu2 (PDB ID:7E9G) for calculations. The TMD method was used to connect the S2 and S3 state. Then, we identified the center of mass of the G_i protein in the optimal binding mode as the initial position and pulled the G_i protein away. From the bulk solvent to the G protein binding site, a total of 20 binding free energies at a 1 Å interval were obtained for each intermediate structure between the S2 and S3 state. Combining these sets of data and the conformational free energy change, we could obtain the free energy landscape that is shown in the main text Figure 5b. The free energy here consists of the conformational free energy of mGlu2-Gi complex and the binding free energy of the two agonists. The possible minimal energy path of how G_i protein couples to mGlu2 is shown in Figure 5b by the black dashed line.

For the GDP release coordinates, we performed series of docking calculations on GDP+Mg^{2+} on each intermediate structure, which was obtained from the possible minimal energy path in Figure 5b at different distances. From nucleotide binding pocket to the bulk solvent, we got 25 binding free energies at a 1 Å interval. Combining these sets of data and the conformational free energy changes, we could obtain the free energy landscape that is shown in the main text Figure 5c.

To evaluate the CG energy, all the all-atomic models we built were relaxed the protein at 50K for 0.2 ns. Our simulations were performed by Molaris-XG package version 9.1.5. The ENZYMIX force field(5, 6) was used. The long-range electrostatics effect was treated by the local reaction field method(7). A gird of unified atoms was used to represent membrane particles and were added to the system by Molaris-XG(5, 6). Then the all-atom structures were converted into the CG representation and performed extensive (5000 steps, 0.001 ps step-size) relaxation at 50K temperature until the energy of system is converged. During relaxation, one structure was output each 100 steps and finally we got a simulation trajectory composed of 50 structures. All these structures were used for energy evaluation. The CG model we used(8-10) focuses on the accurate treatment of the electrostatic and is sensitive to the charge distribution of the protein ionized groups. In consequence, before energy evaluation, a Monte Carlo proton transfer (MCPT) method (9) was used to determine the charge states of the ionizable residues in each structure. During MCPT, protons were "jumped" between ionizable residues, and a standard Metropolis criterion was utilized to calculate the acceptance probability.

S1.2 Targeted Molecular Dynamics

Targeted molecular dynamics was employed to generate the intermediate conformations between the three endpoint states (the S1, S2 and S3 states). During TMD simulation, for each mapping frame m, the mapping is performed, and the system is restrained around the coordinate $r_{0,m}$.

$$r_{0,m} = r_{m-1}^{avg} + \lambda(r_{target} - r_m^{avg}) \quad \text{(S1)}$$

In the equation S1, r_{m-1}^{avg} is the average coordinate of the system in the $m-1$ mapping

frame. r_{target} represents the coordinate of the target protein system. λ is the mapping parameter, $\lambda \in [0,1]$. For the initial frame, r_{m-1}^{avg} is the coordinate of the initial protein system. During TMD simulations, subset of atoms is guided towards a final 'target' structure by means of steering forces. At each step, the root-mean-square (RMS) distance between the current coordinates and the target structure is calculated (after first aligning the target structure to the current coordinates). When the system is restrained at the coordinate $r_{0,m}$, The force on each atom is given by the gradient of the potential:

$$U_{TMD} = k(r - r_{0,m})^2 \quad \text{(S2)}$$

$$k = \frac{1}{2}\frac{k_{spring}}{N} \quad \text{(S3)}$$

In this equation, r is the instantaneous coordinate in the m mapping frame. $r_{0,m}$ evolves linearly from the initial RMS distance at the first TMD step to the target RMS distance at the last TMD step. k is the force constant, which is the ratio of the spring constant k_{spring} and the number of targeted atoms N.

The RMS distance for the system from its current coordinate to the target is shrinking monotonously during the TMD simulation, driving the moving structure toward the target configuration(11). For each domain, forces on the atoms are calculated independently from the other domains.

In our study, from the initial to the target protein system,500 frames of restrained relaxation run were performed. k was set as 100 kcal/mol/Å^2. We picked 15 structures at the equal interval to calculate the free energy profiles of the conformational changes in Figure 5a.

S1.3 Coarse-Grained(CG) model

The coarse-grained model used in this work is one of most reliable models for studying complex protein system like membrane proteins. In this CG models the sidechain of a protein residue is represented as a simplified united atom, whereas the main chain atoms are represented explicitly as shown in Figure S1. The simplified united atom is generally placed at the mass center of the sidechain (for polar and nonpolar residues) or at the center of the charged group of a residue (for ionizable residues). In our CG model, the solvent is treated implicitly and to represent a membrane a grid of effective atoms is used. A consistent treatment of the electrostatic free energy is a key factor for the success of this CG model in explaining the energetics of many complicated and large biological systems (12-14).

The total energy of our CG model is given by the expression:

$$\Delta G_{fold} = \Delta G_{main} + \Delta G_{side} + \Delta G_{main-side}$$
$$= c_1 \Delta G_{side}^{vdW} + c_2 \Delta G_{solv}^{CG} + c_3 \Delta G_{HB}^{CG} + \Delta G_{side}^{elec} + \Delta G_{side}^{polar} + \Delta G_{side}^{hyd} + \Delta G_{main-side}^{elec} \quad \text{(S4)}$$

The terms on the right are the side chain van der Waals energy, main chain solvation energy, main chain hydrogen bond energy, side chain electrostatic energy, side chain polar energy, side chain hydrophobic energy, main chain/side chain electrostatic energy, and main chain/side chain van der Waals energy, respectively. The constants c_1, c_2, and c_3 are scaling coefficients and they have values of 0.10, 0.25, and 0.15, respectively, in this work(15, 16).

S1.4 Semi-microscopic Version of Protein Dipole Langevin Dipole Method (PDLD/S-LRA/β) of Solvation Free Energy and Binding Free Energy Calculation

The free energy of agonist binding was calculated by the PDLD/S-LRA/β method(17-19). The Scaled Protein Dipole Langevin Dipole (PDLD/S) is a method to calculate the electrostatic energies of a system in a semi-microscopic level. In the PDLD calculations,

the solvent molecules are represented by a grid of Langevin dipoles (LD). The LD representation of solvent considers average polarization of the solvent, whereas to use averaged protein configurations multiple snapshots of protein configurations are taken from a long molecular dynamic simulation. Linear response approximation (LRA) is applied to average polarization, and the linear interaction method (LIE) approximates the non-electric binding contribution by a scaled vdW term. Therefore, the overall method was named PDLD/s-LRA/β. Here, we have used the PDLD/s-LRA/β to calculate the solvation and binding free energies of a macromolecular system. The details of the method are discussed in many of our previous works(17, 18). We employed the POLARIS(6) module of Molaris-XG software to calculate the binding free energy of an agonist. The following equation represents the free energy change:

$$\Delta G_{bind}^{PDLD/S-LRA/\beta} = \frac{1}{2}\left(\langle U_{elec,l}^{p}\rangle l - \langle U_{elec,l}^{w}\rangle l\right) + \frac{1}{2}\left(\langle U_{elec,l}^{p}\rangle l' - \langle U_{elec,l}^{w}\rangle l'\right) + \beta\left(\langle U_{vdW,l}^{p}\rangle l - \langle U_{vdW,l}^{w}\rangle l\right) \quad \text{(S5)}$$

where $\langle U_{elec,l}^{p}\rangle l$ is the electrostatic contribution for the interaction between the ligand and its surroundings. p and w designate protein and water, respectively. l and l' designate the ligand in its actual charged form and the "non-polar" ligand, where all of the residual charges are set to 0. Previously, this method was called LRA/α, but since the new element is the β term relative to our original LRA treatment, we prefer the name LRA/β(19).

S1.4 Pathway Search of Agonists Binding to mGlu2 Based on the Free Energy Landscape

In order to reveal the role of agonists during the activation process of mGlu2 (scenario 3 in Figure S3), we take four parameters into consideration: the conformations of L subunit and R subunit, the agonists' positions with respect to L and R subunit. Details are described in Section S1.1. Based on the free energy landscape we obtained (Figure 4 in the main text), the optimal conformational change pathway was sampled using the Monte Carlo sampling(20) as shown in Figure S10. The main process is as follows:

(1) The scaling process is performed to reconstruct the free energy landscape by accelerated molecular dynamics simulation (AMD) method(21-23) in red section of Figure S10. In detail, the new free energy value (E_S') for the conformations of mGlu2 was scaled based on the original free energy value (E_S) as follows:

$$\alpha = E_S(max)\text{-}E_S(min) \quad \text{(S6)}$$

$$E_S' = E_S + \frac{[E_S(max)-E_S]^2}{\alpha+E_S(max)-E_S} = E_S + \frac{[E_S(max)-E_S]^2}{2E_S(max)-E_S(min)-E_S} \quad \text{(S7)}$$

where α is a tuning parameter that determines how deep we want the modified potential energy basin to be. $E_S(max)$and $E_S(min)$ indicate the maximum and minimum energy values in the original free energy landscape.

(2) The sampling process is performed to search possible pathways via the Metropolis sampling process in green block of Figure S1

(3) . The conformational pathways starts at S(0, 0, 0, 0) and ends at S(16,16, 25, 25). The movement of conformational sate for each subunit could be set as -1, 0, and +1, which

means one step backward, staying, and forward respectively. The probabilities for the movement of one subunit should satisfy the following expression:

$$P_{-1} + P_0 + P_{+1} = 1 \quad \text{(S8)}$$

In this study, P_{-1}, P_0, P_{+1} are set with values of 0.2, 0.4, and 0.4 respectively. The entire move of the conformational state for mGlu2 could further be depicted as $M(i,j,l,k)$, $i,j,l,k \in [+1,0,-1]$. The probability for the movement of four subunits can be calculate as follows

$$P_M = P_i * P_j * P_l * P_k \quad \text{(S9)}$$

Each move selection was made randomly based on its relatively probability among all potential move ensemble by normalization. Then, a new conformational state of mGlu2 can be achieved after the move selection. The acceptance of the new conformational state is based on the free energy barriers according to the Monte Carlo method as follows:

$$rand(0,1) \leq exp\frac{-\Delta E}{k_B T} \quad \text{(S10)}$$

(4) The selection process is to evaluate the sampled pathways in yellow part of Figure S11. 5,000 conformational pathways are sampled under the Metropolis criteria. For all the sampled conformational pathways, the redundant conformations that occurring more than twice were deleted from the original pathway. The truncated pathways with no redundant conformations were applied for further processing. Then the free energy barrier calculation for each truncated pathway by considering all the occurred free energy barriers along the pathway. The largest free energy barrier was recorded. Next, we compared the free energy barriers of each truncated pathway and found one which had the smallest energy barrier. Finally, we obtained the energetic and conformational changes along the optimal conformational pathway of agonist binding to VFT in mGlu2 from S1 to S2 process.

In addition, we also considered two other situations shown in Figure S3: only one agonist binds to the L and R subunit (scenario 1 and scenario 2 in Figure S3) respectively. And the process of finding the optimal conformational change pathway in those two situations is similar to the above, the workflow chart is shown in Figure S11.

Different values of P_{-1}, P_0, P_{+1} takes different time for sampling, especially the larger the value of P_{-1}, the longer it takes. Therefore, considering efficiency, the values of P_{-1}, P_0, P_{+1} are 0.2, 0.4, and 0.4 in the scenario that only one agonist binding to the L subunit of mGlu2 dimer while the value of P_{-1}, P_0, P_{+1} are 0.1, 0.45, and 0.45 in the scenario that only one agonist binding to the R subunit of mGlu2 dimer.

Table S1. Conformational free energy terms of key conformations in the process of a conformational transition from the S1 to the S2 state. The unit of energy is kcal/mol.

	$E_{Form2MC}$[1]	$E_{Scaled\ size}$[2]	E_{Hydro}[3]	E_{vdW}[4]	$E_{-DG\ UF}$[5]	E_{Polar}[6]	E_{total}[7]
S1	89.38	258.5	-870.2	-21.43	3.19	52.77	-487.79
I1	79.89	258.5	-863.02	-21.8	3.19	41.59	-501.65
T1	75.06	258.5	-845.91	-21.69	3.19	42.2	-488.65
I2	70.14	258.5	-864.05	-22.29	3.19	44.58	-509.93
T2	81.5	258.5	-845.76	-22.1	3.19	47.49	-477.18
I3	88.47	258.5	-876.07	-22.3	3.19	57.48	-490.73
S2	92.19	258.5	-864.33	-22.08	3.19	53.86	-478.67

[1]: Electrostatic energy term obtained using whole residue charges (0 or ±1), which minimize electrostatic energy in the MCPT method.

[2]:Empirical term that takes into account effect of a protein size on a folding free energy.

[3]:Scaled hydrophobic energy term.

[4]:Scaled van der Waals energy term.

[5]:Negative of a scaled charge-charge energy estimate of an unfolded protein.

[6]:Polar energy contribution term

[7]:The sum of $E_{Form2MC}$, $E_{Scaled\ size}$, E_{Hydro}, E_{VDW}, $E_{-DG\ UF}$ and E_{POLAR}.

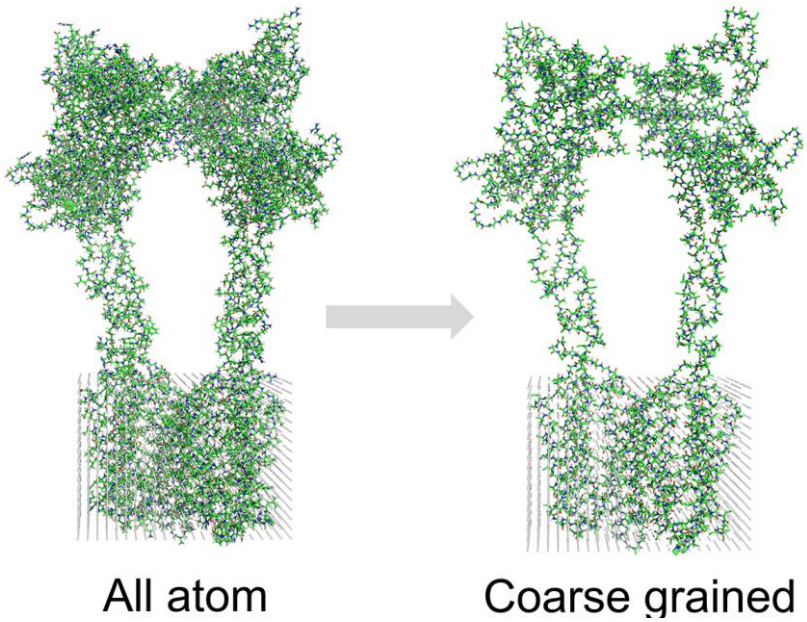

Figure S1. A visual presentation of the CG model used in this study. The inactive state of mGlu2 of PDB 7EPA is shown in an all-atom representation in the left and in a CG representation on the right.

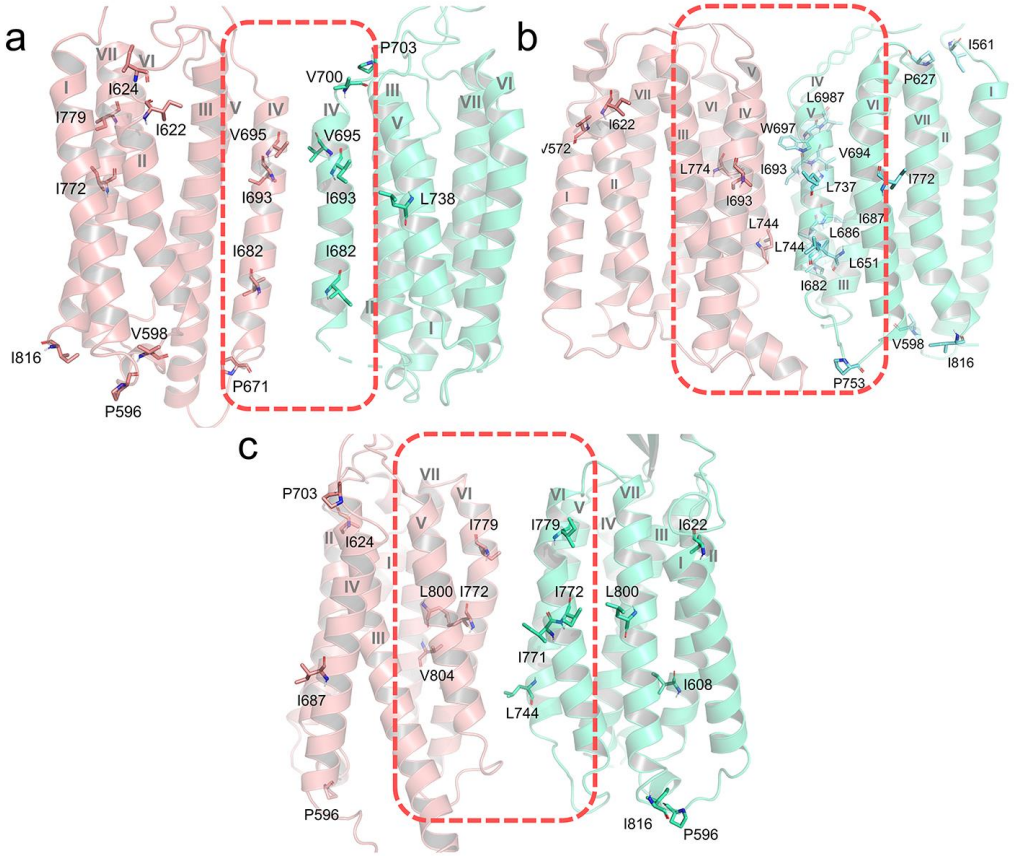

Figure S2. Distribution of key amino acid residues that affect the energy barrier between (a) I1 and T1 state; (b) I2 and T2 state; (c) I3 and S2 state.

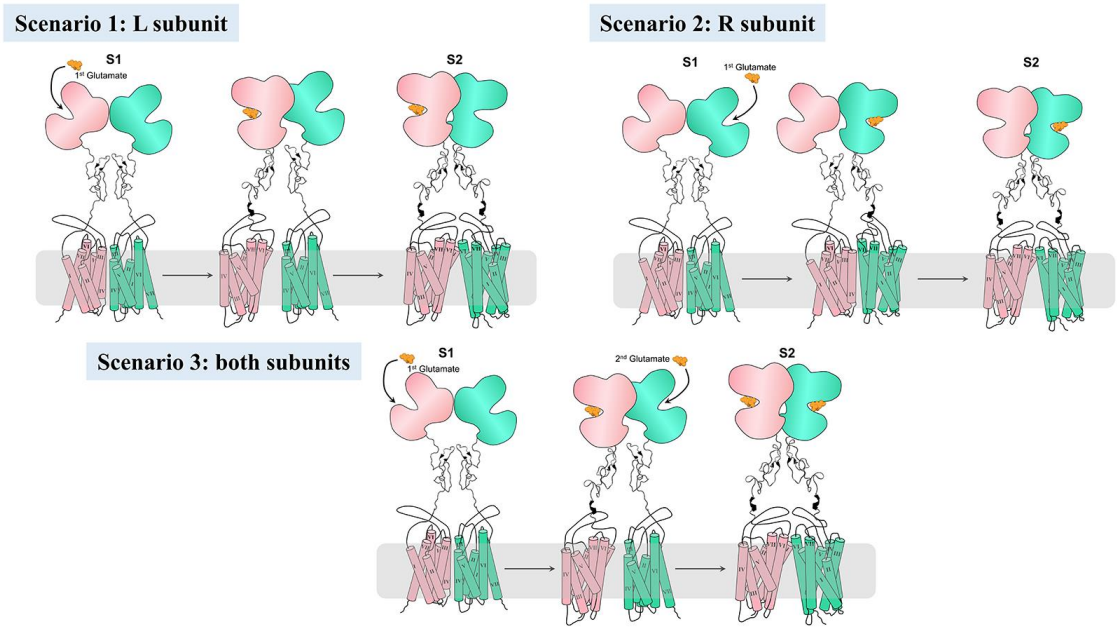

Figure S3. Schematic diagram of glutamate binding to VFT in mGlu2 under three different conditions: with glutamate only binding to the L subunit, with glutamate only binding to the R subunit, with 2 glutamates binding to the L and R subunits.

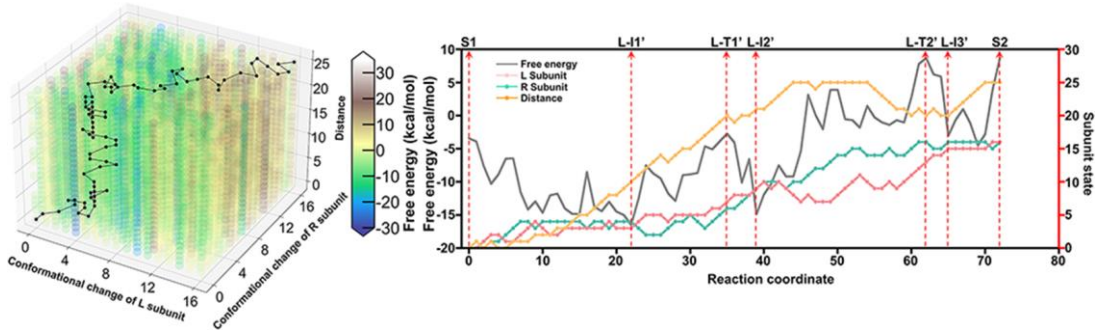

Figure S4. The complete free energy landscape of mGlu2 conformational transition between S1 and S2 states when only the L subunit binds one agonist. (a) Coupled free energy landscape of the distance between the binding pockets in the VFT domain and the agonist and the conformational changes of the L subunit of mGlu2 from state S1 to S2. Totally 17*17*26 states of mGlu2 constructed the complete free energy landscape of the agonist binding process. The X and Y axis indicate the conformational changes of L and R subunits of the mGlu2 dimer which vary from 0 to 16 while the Z axis represents the distance between the binding pocket of the L subunits and the agonist which varies from 0 to 25. The possible minimal energy path is represented by a black line. (b) The key energetic and conformational change along the optimal conformational pathway of agonist binding to VFT in mGlu2 transitioning from S1 to S2 state. Distance here indicates the distance between the ligand and the binding pocket in the VFT domain of the L subunit. The state of L subunit, R subunit, and the distance are represented by pink, green lines, and orange lines, respectively. The highest barrier along this possible minimal energy path is 23.55 kcal/mol, which occurs between the L-I2' and L-T2'.

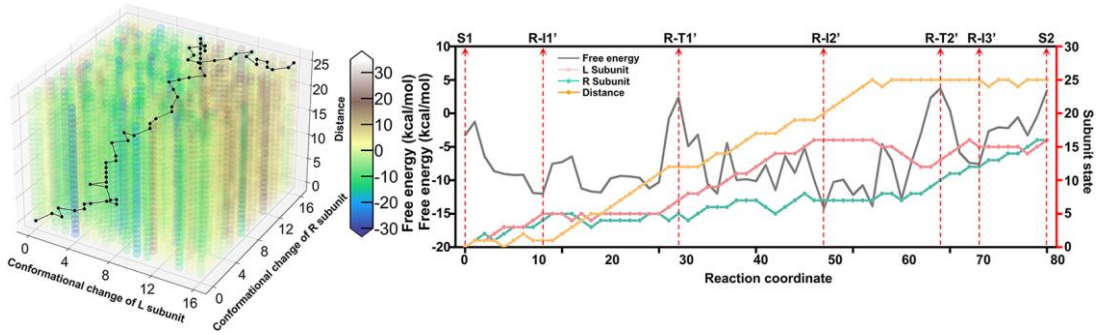

Figure S5. The complete free energy landscape of mGlu2 when only the R subunit binds one agonist. (a) Coupled free energy landscape of the distance between the binding pockets in the VFT domain and the agonist and the conformational changes of the R subunit of mGlu2 from state S1 to S2. Totally 17*17*26 states of mGlu2 constructed the complete free energy landscape of the agonist binding process. The X and Y axis indicate the conformational changes of L and R subunits of the mGlu2 dimer which vary from 0 to 16, while the Z axis represents the distance between the binding pocket of the R subunit and the agonist which varies from 0 to 25. The possible minimal energy path is represented by a black line. (b) The key energetic and conformational change along the optimal conformational pathway of agonist binding to VFT in mGlu2 transitioning from S1 to S2 state. Distance here indicates the distance between the ligand and the binding pocket in the VFT domain of the R subunit. The state of L subunit, R subunit, and the distance are represented by pink, green, and orange lines, respectively. The highest barrier along this possible minimal energy path is 17.90 kcal/mol, which occurs between the R-I2' and R-T2'.

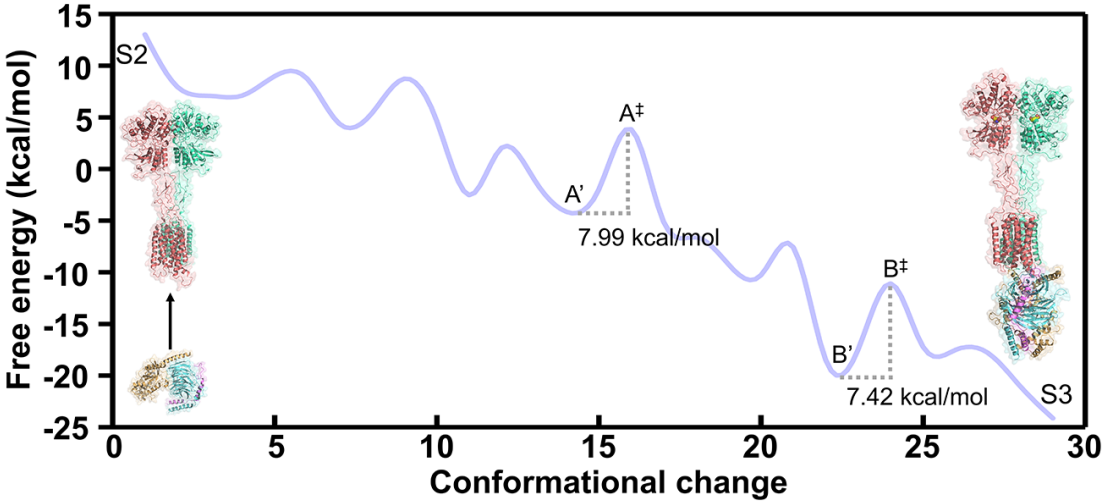

Figure S6. Free energy profiles along the minimal energy path in Figure 5b during the G_i coupling to mGlu2 activation process.

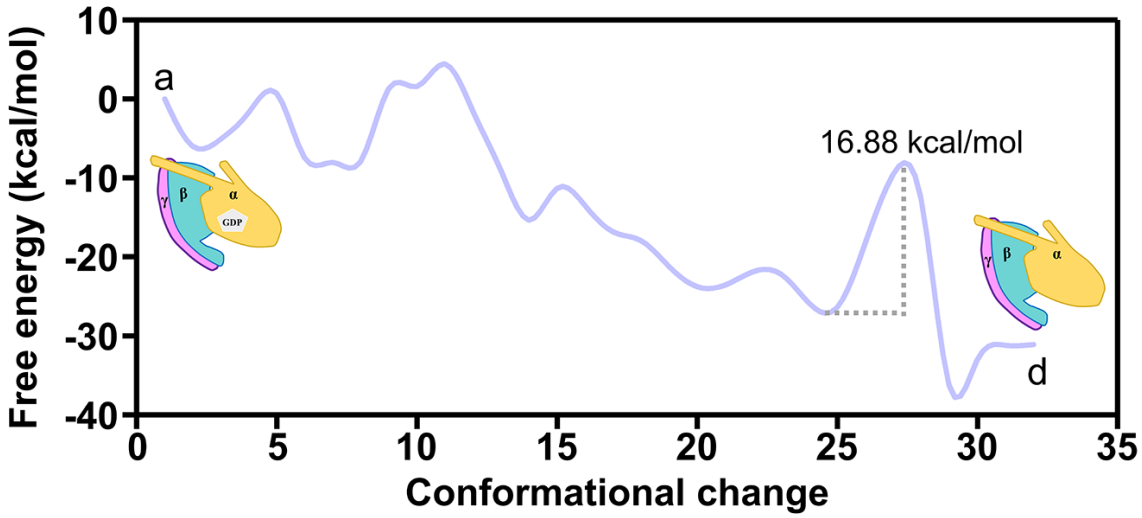

Figure S7. Free energy profiles along the minimal energy path (Path 3 in Figure 5c, from potin a to point d) during the GDP release process.

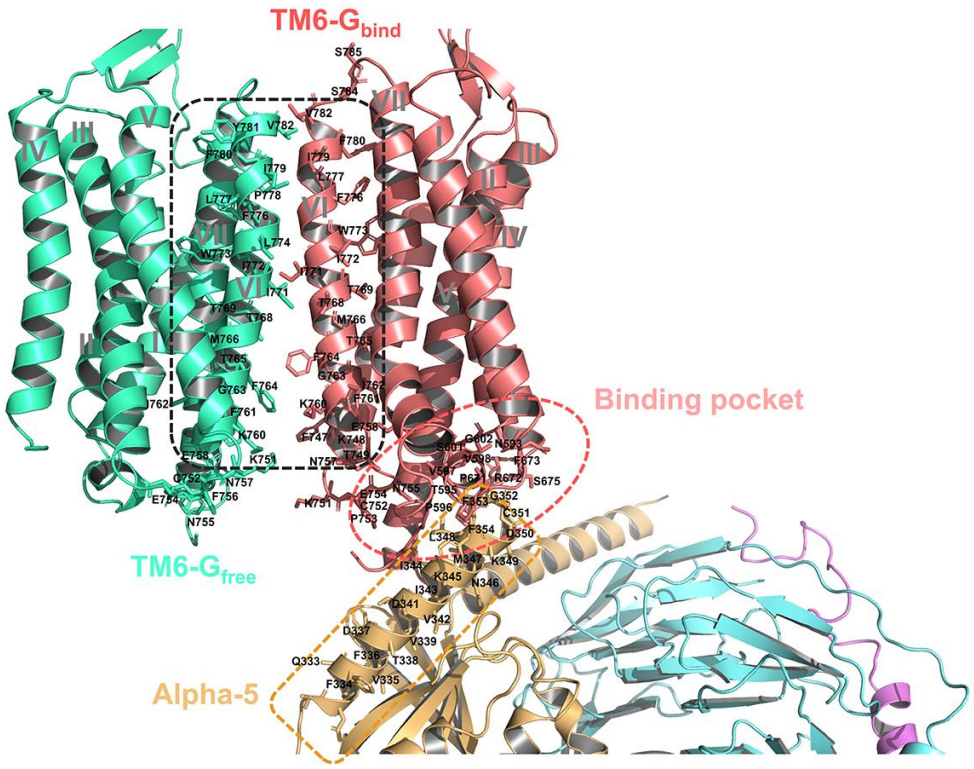

Figure S8. Distribution of key residues in mGlu2-G_i complex.

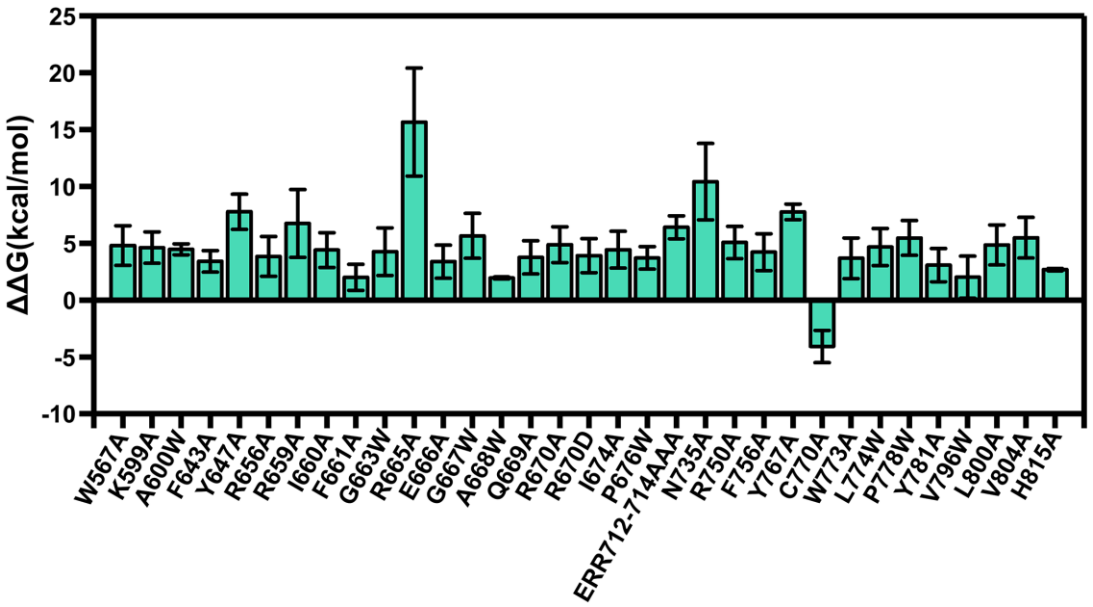

Figure S9. Evaluation of mutational effects of the key residues identified by previous studies. The effects were calculated using $\Delta\Delta G = \Delta G_{mutant} - \Delta G_{WT}$. $\Delta\Delta G > 0$ indicates the mutation impedes G_i activation, and $\Delta\Delta G < 0$ indicates the mutation facilitates G_i activation. The data are expressed as means ± SEM.

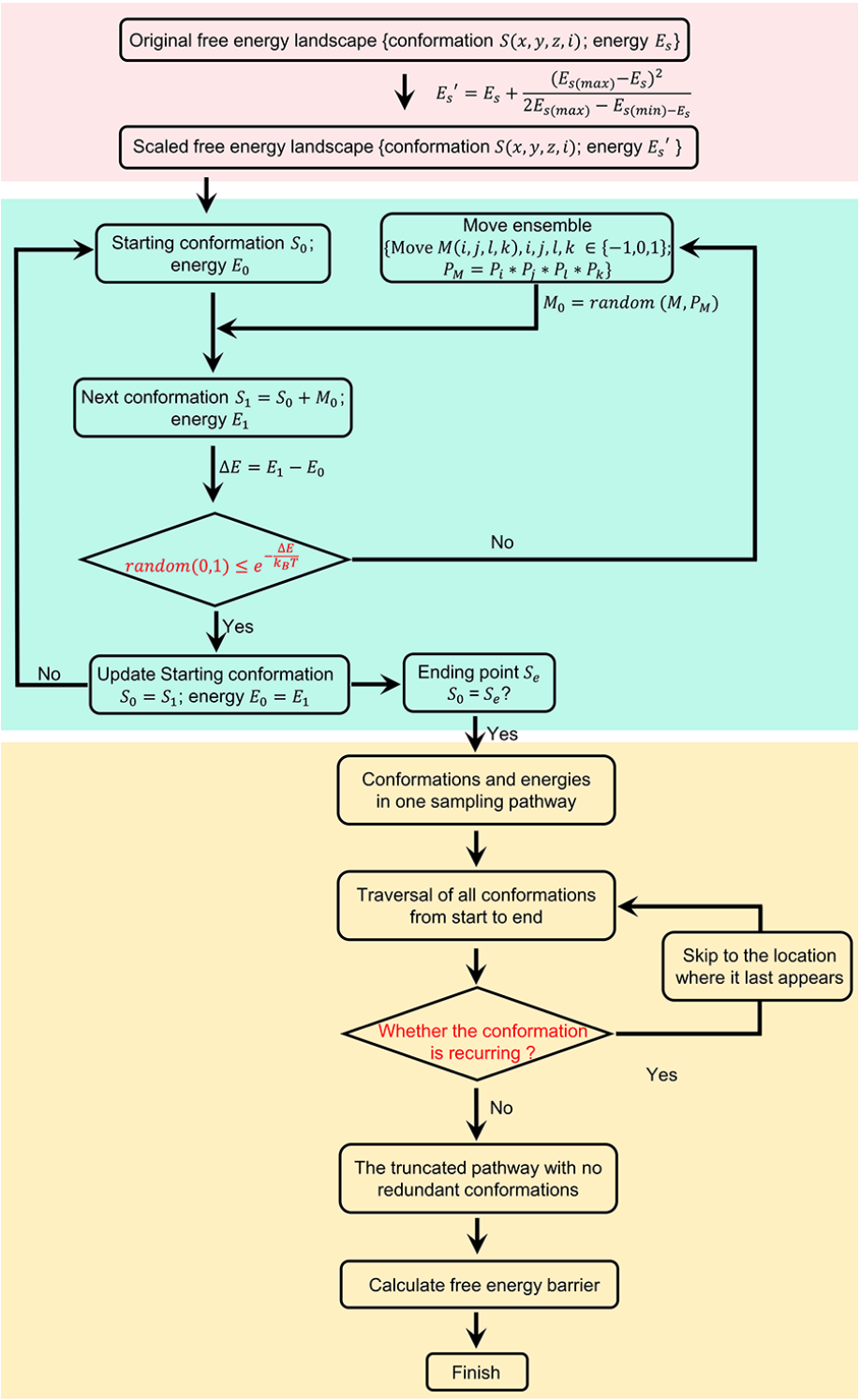

Figure S10. Flowchart of finding the optimal energy path, and conformational changes of agonists binding to two VFTs in the mGlu2 dimer. In red section, the scaling process is performed to reconstruct the free energy landscape by accelerated molecular dynamics simulation (AMD) method. In green section, the sampling process is performed to search possible pathways via the Metropolis sampling process. Totally 5,000 conformational pathways are sampled under the Metropolis criteria. And in yellow section, the selection process to evaluate the sampled pathways is shown.

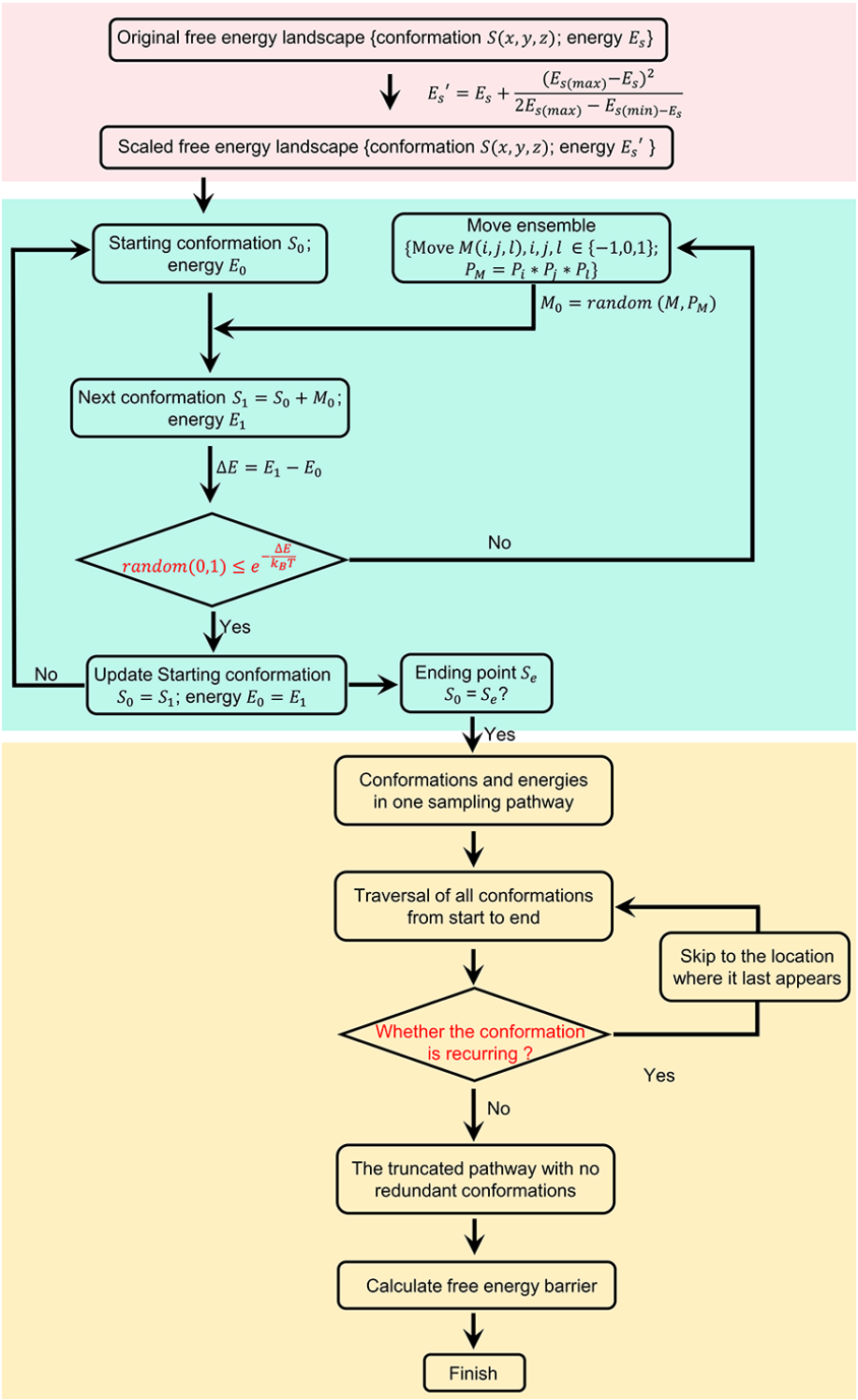

Figure S11. Flowchart of finding the optimal energy path, and conformational changes of an agonist only binding to the VFT in one subunit of mGlu2. In red section, the scaling process is performed to reconstruct the free energy landscape by accelerated molecular dynamics simulation (AMD) method. In green section, the sampling process is performed to search possible pathways via the Metropolis sampling process. Totally 5,000 conformational pathways are sampled under the Metropolis criteria. And in yellow section, the selection process to evaluate the sampled pathways is shown.

References

1. E. F. Pettersen *et al.*, UCSF Chimera—a visualization system for exploratory research and analysis. *Journal of computational chemistry* **25**, 1605-1612 (2004).
2. M. A. Martí-Renom *et al.*, Comparative protein structure modeling of genes and genomes. *Annual review of biophysics and biomolecular structure* **29**, 291-325 (2000).
3. B. Webb, A. Sali, Comparative protein structure modeling using MODELLER. *Current protocols in bioinformatics* **54**, 5.6. 1-5.6. 37 (2016).
4. Y. Yan, H. Tao, J. He, S.-Y. Huang, The HDOCK server for integrated protein–protein docking. *Nature protocols* **15**, 1829-1852 (2020).
5. S. C. Kamerlin, S. Vicatos, A. Dryga, A. Warshel, Coarse-grained (multiscale) simulations in studies of biophysical and chemical systems. *Annual review of physical chemistry* **62**, 41-64 (2011).
6. F. S. Lee, Z. T. Chu, A. Warshel, Microscopic and semimicroscopic calculations of electrostatic energies in proteins by the POLARIS and ENZYMIX programs. *Journal of Computational Chemistry* **14**, 161-185 (1993).
7. F. S. Lee, A. Warshel, A local reaction field method for fast evaluation of long‐range electrostatic interactions in molecular simulations. *The Journal of chemical physics* **97**, 3100-3107 (1992).
8. S. Vicatos, A. Rychkova, S. Mukherjee, A. Warshel, An effective coarse-grained model for biological simulations: recent refinements and validations. *Proteins* **82**, 1168-1185 (2014).
9. I. Vorobyov, I. Kim, Z. T. Chu, A. Warshel, Refining the treatment of membrane proteins by coarse-grained models. *Proteins* **84**, 92-117 (2016).
10. M. Lee, V. Kolev, A. Warshel, Validating a Coarse-Grained Voltage Activation Model by Comparing Its Performance to the Results of Monte Carlo Simulations. *J Phys Chem B* **121**, 11284-11291 (2017).
11. J. Schlitter, M. Engels, P. Krüger, Targeted molecular dynamics: A new approach for searching pathways of conformational transitions. *Journal of Molecular Graphics* **12**, 84-89 (1994).
12. C. Bai, M. Asadi, A. Warshel, The catalytic dwell in ATPases is not crucial for movement against applied torque. *Nature Chemistry* **12**, 1187-1192 (2020).
13. C. Bai, A. Warshel, Revisiting the protomotive vectorial motion of F0-ATPase. *Proceedings of the National Academy of Sciences* **116**, 19484-19489 (2019).
14. S. Mukherjee, A. Warshel, Dissecting the role of the γ-subunit in the rotary–chemical coupling and torque generation of F1-ATPase. *Proceedings of the National Academy of Sciences* **112**, 2746-2751 (2015).
15. C. Bai *et al.*, Exploring the activation process of the β2AR-Gs complex. *Journal of the American Chemical Society* **143**, 11044-11051 (2021).
16. S. Vicatos, A. Rychkova, S. Mukherjee, A. Warshel, An effective Coarse‐grained model for biological simulations: Recent refinements and validations. *Proteins: Structure, Function, and Bioinformatics* **82**, 1168-1185 (2014).
17. I. Muegge, H. Tao, A. Warshel, A fast estimate of electrostatic group contributions to the free energy of protein-inhibitor binding. *Protein engineering* **10**, 1363-1372 (1997).
18. C. N. Schutz, A. Warshel, What are the dielectric “constants” of proteins and how to

validate electrostatic models? *Proteins: Structure, Function, and Bioinformatics* **44**, 400-417 (2001).

19. N. Singh, A. Warshel, Absolute binding free energy calculations: on the accuracy of computational scoring of protein–ligand interactions. *Proteins: Structure, Function, and Bioinformatics* **78**, 1705-1723 (2010).
20. G. Kuczera, E. Parent, Monte Carlo assessment of parameter uncertainty in conceptual catchment models: the Metropolis algorithm. *Journal of hydrology* **211**, 69-85 (1998).
21. C. A. F. de Oliveira, D. Hamelberg, J. A. McCammon, Coupling accelerated molecular dynamics methods with thermodynamic integration simulations. *Journal of chemical theory and computation* **4**, 1516-1525 (2008).
22. P. C. Gedeon, J. R. Thomas, J. D. Madura, Accelerated molecular dynamics and protein conformational change: a theoretical and practical guide using a membrane embedded model neurotransmitter transporter. *Molecular modeling of proteins*, 253-287 (2015).
23. D. Hamelberg, J. Mongan, J. A. McCammon, Accelerated molecular dynamics: a promising and efficient simulation method for biomolecules. *The Journal of chemical physics* **120**, 11919-11929 (2004).